2020

Review—Single Walled Carbon Nanotubes as Optical Sensors for Biological Applications

Eric M. Hofferber
University of Nebraska - Lincoln, Hofferber.Eric@gmail.com

Joseph A. Stapleton
University of Nebraska - Lincoln, JStapleton346@gmail.com

Nicole M. Iverson
University of Nebraska - Lincoln, iverson@unl.edu

Review—Single Walled Carbon Nanotubes as Optical Sensors for Biological Applications

Journal of The Electrochemical Society, 2020 **167** 037530

Review—Single Walled Carbon Nanotubes as Optical Sensors for Biological Applications

Eric M. Hofferber, Joseph A. Stapleton, and Nicole M. Iverson[*,z]

Department of Biological Systems Engineering, University of Nebraska-Lincoln, Lincoln, Nebraska 68583, United States of America

Since the discovery of the band gap fluorescence from single walled carbon nanotubes (SWNT) many advancements have been made towards the use of these unique fluorophores as optical biosensors in vitro, ex vivo in vivo. Attention has been given to these pure carbon structures due to their photostability, tunable properties, and bright near infrared emission that falls in the tissue transparency window. This review highlights some of the major advancements in the field of SWNT biosensors over the last two decades with a focus given to recent advances in biological applications.

 [DOI: 10.1149/1945-7111/ab64bf]

Manuscript submitted September 19, 2019; revised manuscript received December 6, 2019. Published January 10, 2020. *This paper is part of the JES Focus Issue on Sensor Reviews.*

Biosensors are unique devices capable of converting biological cues into signals for detection and analysis.[1] Such devices are capable of expanding current knowledge of biological pathways by informing researchers of key analytes that are involved in processes, core molecular signaling pathways, and deviations from homeostasis that are consistent with disease states.[2] The expansion of knowledge gained by the use of biosensors could lead to earlier disease detection and more targeted therapies.[2] Since the first paper using the term "biosensor" by Cammann in 1977, a paper that predominantly discussed work performed using enzyme-based detection,[3] the field of biosensors has come to describe many more types of sensors, including cell or tissue-based, immuno, DNA, magnetic, thermal, piezoelectric, and optical sensors.[1,4–10] Yet, despite the variety of biosensors developed over the last four decades, the same key qualities are consistently found: stability, high specificity for a target, biocompatibility, and limited nonspecific binding.[11–16]

Of the aforementioned biosensors, optical biosensors have generated a great deal of interest in recent years due to their high sensitivity, rapid detection rate, non-invasive nature, and non-destructive method of action.[17–19] The previously mentioned characteristics coupled with the ability of optical biosensors to detect a wide variety of analytes has led to research targeted at expanding this branch of biosensors over the last two decades.[20] Recently, a push to move optical biosensors into the near infrared (nIR) region of the electromagnetic spectrum has gained a great deal of traction.[21–25] Many optical biosensors or fluorescent probes require excitation in the low end of the visible spectrum or even in the ultraviolet (UV) region, which can limit sensor timeframes due to photobleaching of organic molecules, and concerns of phototoxicity arise when UV light is used on biological matter.[26–33] UV and visible light are also obstructed by biological tissues due to reflection, absorption, and scattering of the light by tissue, water, and blood.[34,35] Consequently, tissue penetration depth for visible light has been estimated at >0.1 cm,[17] but as the wavelengths move toward the nIR spectrum, tissue penetration increases.[21–23,25,34,36,37] For the nIR-I (780–900 nm) and nIR-II (900–1700 nm) regions, light is capable of penetrating tissue at depths of up to 1 cm and 3 cm respectively.[38,39] The increase in tissue penetration depth that is observed with nIR wavelengths is attributed to off resonance frequency of the light compared to water, blood, and tissue, which leads to less absorption and scattering.[40]

Of the nIR optical biosensors, carbon nanotubes (CNT) have been studied at length.[41–46] Conceptually, a single walled carbon nanotube (SWNT) is a sheet of pure graphene that has been rolled into a tube that is approximately 1 nm in diameter.[47] SWNT are quasi one-dimensional nanowires with typical lengths varying from 10 nm to a few hundred nanometers,[47] however the length can be much longer with some nanotubes measuring over 50 cm.[48] The orientation of the fully sp2-bonded carbon hexagonal rings determines the helicity of the nanotube and is denoted by two integers (n, m) that are referred to as the chiral indices (as shown in Fig. 1).[49–52] When the value of m is zero the nanotube is in a zigzag structure, when the values of n and m are equal the nanotube is in an armchair structure, when n and m are different the nanotube is in a chiral structure.[49–51] Zigzag, armchair, and chiral nanotubes act very differently and are classified either semiconducting, metallic, or semi metallic.[49–51,53] Nanotubes have a small enough diameter to be subject to the quantum confinement effect, which states that the electrons can only exist in discrete energy levels.[54] The band gap between semiconducting SWNT electrons is on the order of 1 eV, which leads to fluorescence in the nIR-II range (900–1700 nm) with excitation typically falling in the nIR-I (780–900 nm) range or in the higher length visible range (>600 nm).[24,54–59] The Stoke-shift between the excitation and emission wavelengths of SWNT leads to a decreased autofluorescence when used for imaging in biological samples, which is another positive factor that is driving the development and use of SWNT as biosensors.[24,51,56,60,61]

Many papers have been published over the last two decades moving towards the use of SWNT as in vitro, ex vivo, and in vivo optical biosensors.[62–74] This review examines the major advancements in SWNT biosensing since the discovery of band gap fluorescence from individual nanotubes in 2002 with a focus on recent progress and future directions.

Major Advances: 2002–2016

SWNT was originally discovered by Sumio Iijima in 1991,[47] however the discovery of the band gap fluorescence that led to the use of SWNT as optical biosensors did not occur until O'Connell et al.'s 2002 paper.[55] O'Connell et al. was able to suspend individual nanotubes in aqueous solutions using sodium dodecyl sulfate (SDS) and poly(vinylpyrrolidone) (PVP) with sheer mixing and tip sonication to form cylindrical micelles around the tubes. The aqueous solution of individual nanotubes was found to brightly fluoresce at distinct wavelengths within the nIR-II range, which piqued the interest of chemists, biologists, and engineers since the tissue transparency window falls in the nIR-II fluorescence range.[55] The 650–1350 nm range has been termed as the tissue transparency window because of the lack of light absorbed by blood or water in these wavelengths (see Fig. 2).[23,75]

*Electrochemical Society Member.
[z]E-mail: iverson@unl.edu

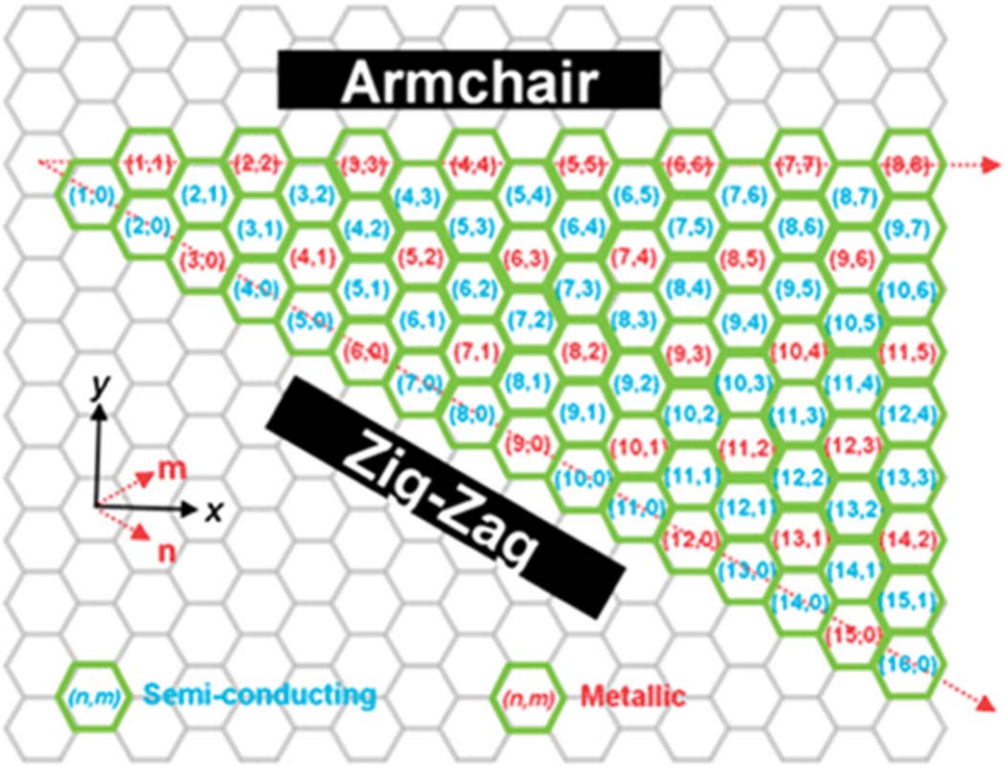

Figure 1. Single walled carbon nanotube properties change with the change in their carbon bond angles. When m is zero the nanotube is a zigzag structure, when n and m are equal the nanotube is an armchair structure, and when n and m are different the nanotube is chiral (figure adapted with permission from 52, © 2012 The Royal Society of Chemistry).

Two years later, in 2004, multiple labs published research that advanced our understanding and ability to use SWNT.[76–78] Lefebvre et al. fabricated SWNT using chemical vapor deposition which resulted in a raw mixture of many different nanotube chiralities.[79,80] A modified microscope was able to image individual SWNT in air and was able to show distinct excitation and emission wavelengths for different chiralities (see Fig. 2),[81] confirming the hypothesis that various SWNT chiralities have different band gaps and therefore distinct excitation and emission wavelengths.[78] Heller et al. separated SWNT in aqueous solution by length and diameter using gel electrophoresis, which enabled sample enrichment with a specific SWNT chirality to increase the overall quantum yield (QY) of the sample.[77] Finally, Cherukuri et al. made the first leap into in vitro imaging with SWNT using mouse macrophage-like cells.[76] As predicted, the long wavelength emission of the SWNT allowed for high signal to noise (s/n) fluorescence detection in the living cells, and the cells were determined to not be adversely affected by the nanotubes under the experimental conditions.

Three years later, in 2007, there was another big step in the use of SWNT as optical biosensors when Leeuw et al. performed the first published in vivo imaging experiment with functionalized SWNT.[82] Drosophila larva were fed a diet containing dispersed SWNT and the viability, size, and fluorescence of the flies was monitored during the drosophila's life cycle. The drosophila did not have significantly different life spans or overall size measurements due to the addition of SWNT, and the SWNT was detectable with nIR imaging in the digestive system of the animals. This research demonstrated the potential for biocompatibility and fluorescence functionality of SWNT in vivo for the first time. Following Leeuw et al.'s demonstration of in vivo detection of SWNT, Welsher et al.

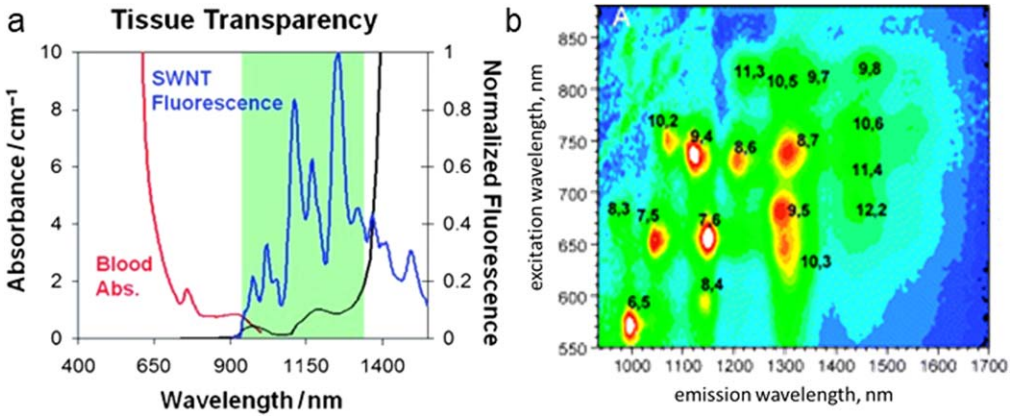

Figure 2. (a) Single walled carbon nanotubes (SWNT) fluorescence within the Tissue Transparency Window, the area between where blood and water absorb light (figure reprinted with permission from 75, © 2011 Wiley-VCH Verlag GmbH & Co. KGaA, Weinheim). (b) Different chiralities of SWNT are excited and emit light at different wavelengths (figure reprinted with permission from 81, © 2006 American Chemical Society).

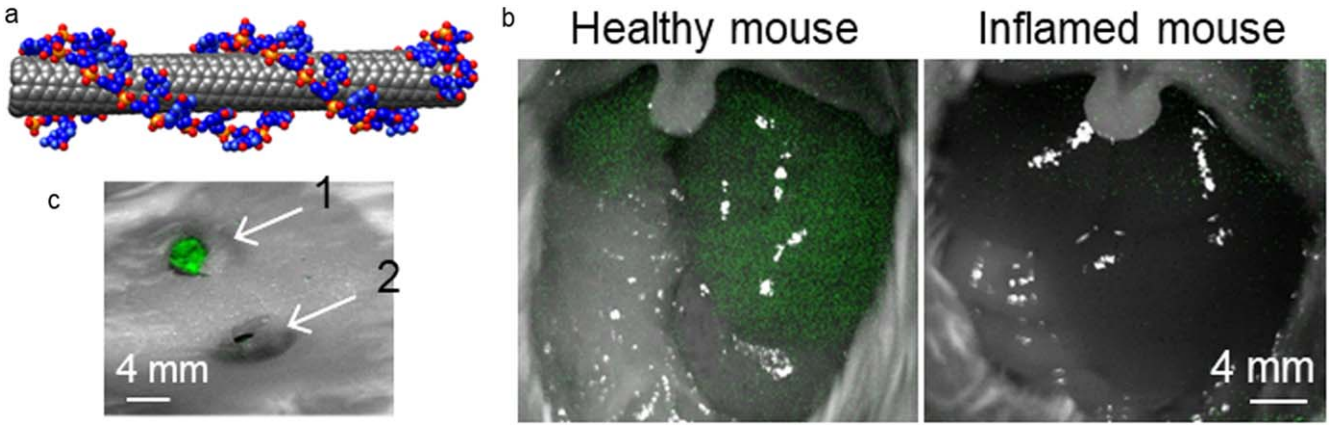

Figure 3. (a) Single walled carbon nanotubes (SWNT) wrapped with single stranded DNA can create fluorescent sensors for various analytes.[20,73,84] (b) SWNT sensors located within the liver show the ability to detect inflammation by through signal quenching.[85] (c) SWNT encapsulated hydrogels placed subcutaneously in a mouse can detect the nitric oxide that is released by cutting the skin (fluorescence is quenched within 30 min of hydrogel placement, image was taken 5 min after gel 1 and 30 min after gel 2 placement).[85]

demonstrated the ability of SWNT to be utilized in live mammals, by injecting polyethylene glycol (PEG) modified SWNT made with the SDS exchange process into mice and imaging the nanotubes throughout the animal.[68] The relative QY of the PEG-SWNT was higher than previously employed SWNT due to the decreased sonication requirements for nanotube dispersion with the exchange method. Researchers found that PEG-SWNT localized to tumors when injected into tumor laden mice, developing a method for high resolution imaging of tumor vasculature.

Cognet et al. advanced the field of SWNT sensors by showing a stepwise quenching of nanotube fluorescence in response to low levels of acid in 2007.[83] By imaging individual nanotubes' interactions with acid, Cognet et al. demonstrated single molecule detection by SWNT. A paradigm shift in SWNT sensors occurred in 2009 when Heller et al. showed the potential for SWNT wrapped with ssDNA to be a multimodal detector by showing simultaneous detection of four pathways using principal component analysis (PCA) (see Fig. 3).[20] Two chiralities of SWNT (6, 5 and 7, 5), when wrapped with ss$(GT)_{15}$, underwent a shift in either wavelength or intensity following exposure to four different analytes. Through the use of wavelengths and intensities gathered from both chiralities PCA was able to detect the presence of multiple analytes at once.

In 2013 SWNT were used as biosensors in live animals for the first time when Iverson et al. demonstrated two methods for in vivo sensor delivery, intravenous and subcutaneous (Fig. 3).[85] Both sensor delivery methods were performed with ssDNA wrapped SWNT that were shown to retain their specificity and functionality in vivo.

Major Advances: 2017–2019

Many advances have been made in the field of carbon nanotube biosensors in the past three years with regards to sensor design and in vitro, ex vivo and in vivo applications. The next sections highlight major advances in each application from the last three years.

Sensor development.—The library of available SWNT based optical biosensors is rapidly expanding each year as scientists are demonstrating high sensitivity and selectivity to biologically active markers and analytes. This section highlights the sensors developed in the past three years.

Catecholamine neurotransmitters, such as dopamine and norepinephrine, have been at the center of SWNT sensor development due to the difficult nature of in situ detection and quantification of analytes in neural networks. Beyene et al. sought to create a more targeted approach to sensor design by testing ssDNA interaction with the neurotransmitters under various conditions to induce an "ultra large" fluorescence modulation for eventual in vivo applications.[86] The developed $(GT)_6$-SWNT sensor was found to show a 3500% fluorescence increase in response to the added neurotransmitters.[86] In a study by Mann et al. the issue of discerning dopamine from norepinephrine was addressed by the fabrication and testing of multiple neurotransmitter SWNT-based sensors to determine which was capable of distinguishing one catecholamine from another.[84] A_{30} and $(GT)_{10}$-SWNT were found to have more sensitivity to dopamine vs other catecholamine neurotransmitters.[84] These increases in fluorescence response and improvement in specificity of SWNT-sensors are both key steps towards the goal of in vivo detection and quantification of neurotransmitters.

Expansion of the SWNT senor library has resulted in different detection methods for target analytes other than the direct interaction of an analyte with SWNT, which leads to a change in the dielectric environment, causing shift in emission wavelength or intensity. Harvey et al. was able to show controlled solvatochromic shifting of nanotube fluorescence in response to alkylating agents commonly used as chemotherapy drugs (see Fig. 4).[87] The alkylating agents covalently bind to the nanotube's DNA wrapping, causing a conformational change in the DNA that exposes more of the SWNT to the surrounding environment.[87] The exposed SWNT was shown to either red or blue shift depending on the medium that was employed.[87] Detection of larger, bioactive proteins has also been an area of interest for SWNT sensing, Lee et al. used aptamer-SWNT and aptamer-anchor-SWNT complexes for insulin sensing.[88] The SWNT was functionalized using aptamers that underwent conformational changes in response to insulin, resulting in a change to the nanotube's dielectric environment.[88] In a similar vein, Zubkovs et al. designed a new sensor platform to detect glucose that did not rely on the addition of exogenous mediators, which limits utility and reversibility of the sensors, as was previously done.[89] Zubkovs et al.'s platform uses enzymatic pocket doping with a glucose oxidase (GOx) wrapping to create a glucose sensor that required no mediator and achieves reversibility of fluorescence response.[89] Oxygenated p-doped sites on the nanotube were shown to decrease nanotube emission while addition of glucose caused oxidation to occur in the GOx wrapping, resulting in n-doping and an overall increase in nanotube emission.[89] Finally, Dong et al. was able to create a lab-on-a-chip-type sensing platform using SWNT sensors conjugated to a microarray for detection and quantification of antibodies.[90] A SWNT/chitosan ink was deposited onto a substrate to form a microarray which was further modified using copper ions and capture proteins. When the analyte of interest interacts with the capture protein the distance from the copper ion to the SWNT is changed, leading to a change in the dielectric environment and a shift in the nanotube fluorescence.[90] This new platform has potential for both antibody and protein sensing applications in the future.

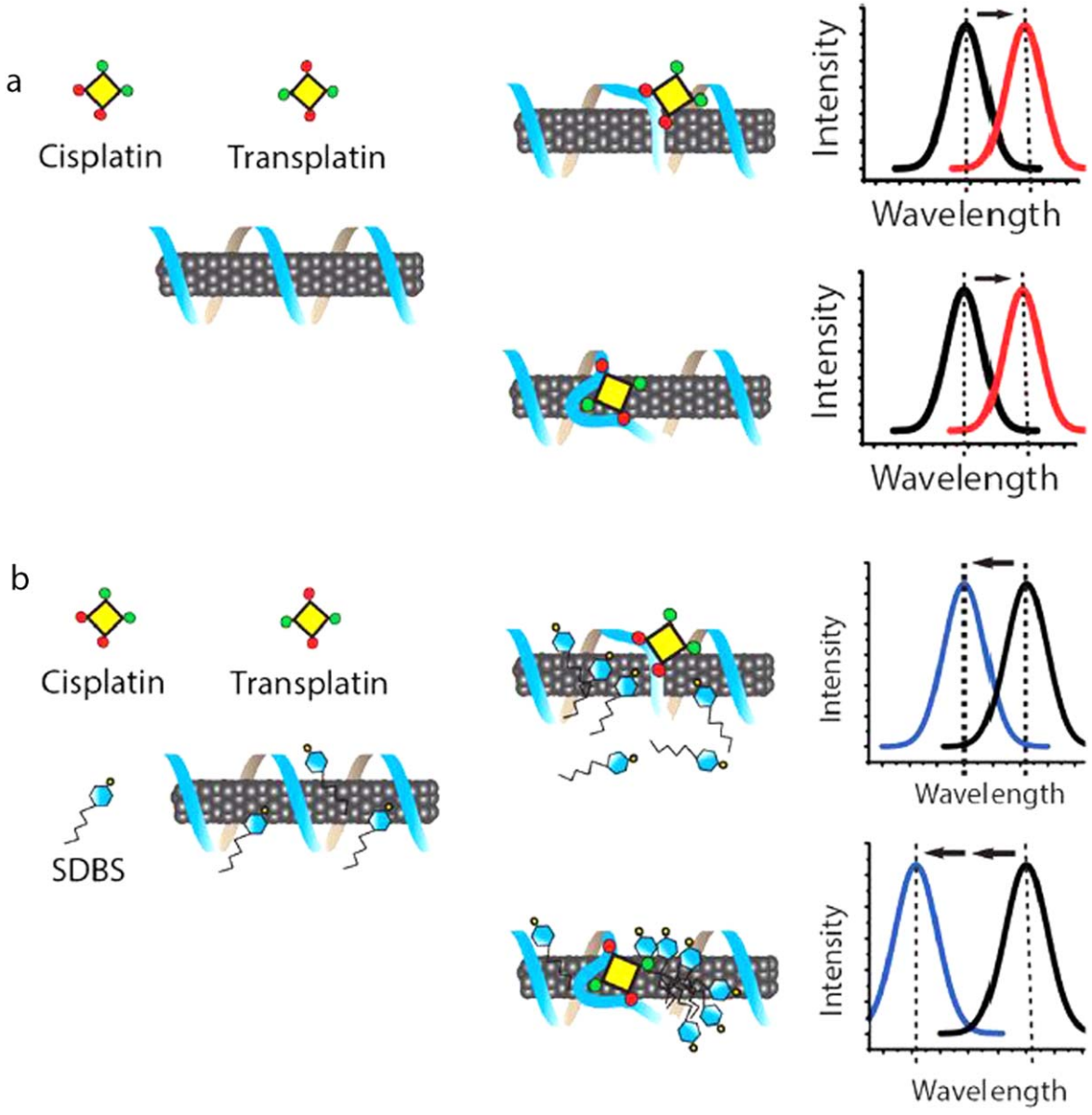

Figure 4. Illustration of the proposed mechanism of the difference in nanotube emission response upon interaction with alkylating agents. (a) Cisplatin and transplatin react with DNA on the nanotube to produce red shifts. (b) When an amphiphile, sodium dodecylbenzenesulfonate (SDBS), is introduced to the system, large blue shifts in the fluorescence take place mediated by the alkylating agents. (figure reproduced with permission from 87, © 2017 American Chemical Society).

In vitro.—In vitro applications of SWNT biosensors have seen recent advances in both intracellular and extracellular applications.[91–94] The next section highlights the recent advances in SWNT sensor research with cell culture.

Delivery of the newly designed SWNT sensors to biological samples continues to be an obstacle in the use of SWNT for biomedical research. One step towards the use of SWNT sensors with biological samples was Kruss et al.'s study detecting dopamine in real time as it was released from neuroprogenitor cells.[91] Kruss et al.'s study showed a high spatial and temporal resolution of dopamine released from cells (shown in Fig. 5) and improved the ability to investigate small changes in analyte concentration in vitro.[91] Along the same lines, Dinarvand et al. used a SWNT aptamer sensor to detect serotonin release from cells with both spatial and temporal specificity.[92] The sensors along the perimeter of the cells allowed for many sites of quantification and could lead to important discoveries in cell to cell signaling.[92] Extracellular protein detection has also seen recent progress with Chio et al.'s 2019 paper, in which peptoid-SWNT assemblies detected lectin protein wheat germ agglutinin in cell culture conditions.[93] The peptoid wrapping was shown to interact with the proteins of interest while the proteins were able to retain function following the interaction.[93] This work paves the way for extracellular detection of complex analytes.

Intracellular detection of analytes by SWNT based optical probes has been hindered by a lack of mechanisms for targeted aggregation of sensors to specific proteins or organelles. Recently, Budhathoki-Uprety et al. showed that guanidinium-functionalized helical polycarbodiimide SWNT entery into HeLa cell nuclei was mediated by the import receptor importin β.[94] The nanotube photoluminescence exhibited distinct red-shifting upon entry to the nucleus, making the sensors a reporter of the importin β-mediated nuclear transport process.[94] This research also shows the potential of using SWNT's own properties to determine the location of the nanoparticles within cells.

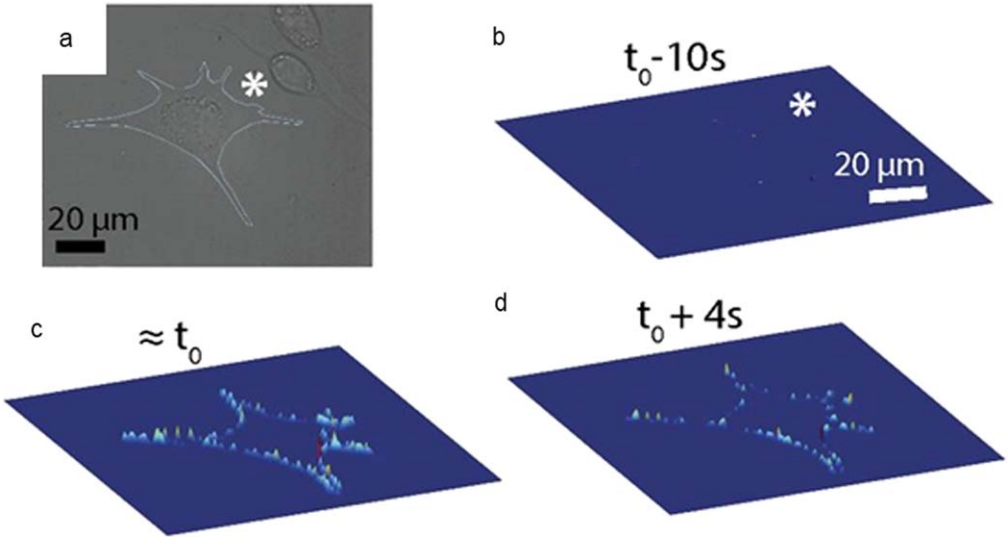

Figure 5. Nanosensor array that allows for real time detection of analyte released from cells[91] (a) brightfield image of cell, (b) heatmap showing analyte concentration before cell stimulation, (c) analyte concentration at stimulation point, and (d) analyte concentration 4 s post stimulation (figure reprinted with permission from 91).

Ex vivo.—Ex vivo detection of biomarkers in biological media (serum, blood, urine, etc) has experienced sensor library expansion, a new immobilization scheme, and improved disease state detection.[95–99]

The development of each SWNT sensor is time intensive, and therefore the library of SWNT sensors is limited. Despite this difficulty, multiple new SWNT sensors have been developed over the past few years for use with biological media.[95–99] Bisker et al. developed an insulin sensor by wrapping 10,6 SWNT with C_{16}-PEG-ceramide polymers.[95] It was found that insulin does not have an affinity to C_{16}-PEG-ceramide when it is not attached to nanotubes, but rather insulin interacts with C_{16}-PEG-ceramide only when it is wrapped around the nanotube. These results suggest that the sensor's response to insulin is due to molecular recognition rather than a measurement of other physical parameters.[95] The C_{16}-PEG-ceramide wrapped SWNT responded to the presence of insulin in both solution and serum through fluorescence quenching.[95] Another protein, RAP1, was detected using aptamers anchored to SWNT by ss$(AT)_{11}$, demonstrating an ability to create SWNT sensors with already existing aptamer technology.[96] The $(AT)_{11}$-RAP1-SWNT sensor responds to the presence of RAP1 with a concentration dependent increase in fluorescence intensity, allowing for single molecule detection of the protein in serum.[96]

A sensor that functions in urine, detecting microalbuminuria, a marker for cardiovascular disease, cancer, metabolic disease, diabetes, hypertension, and atherosclerosis was developed by Budhathoki-Uprety et al. in 2019.[97] Carboxy-polycarbodiimide (PCD) wrapped 9,4 SWNT shows a concentration dependent signal change in response to the presence of microalbuminuria and incorporation into a nanosensor paint allows for portability of a nanosensor array.[97] The use of the carboxy-PCD-SWNT complexes in urine expands the use of SWNT sensors into human samples and the development of a nanosensor paint allows for readings outside of laboratory settings.

Detection of disease specific markers or direct virus detection has also been shown in biological media in recent years.[98,99] Williams et al. developed a SWNT sensor for a metastatic prostate cancer marker, specifically urokinase plasminogen activator (uPA), in human blood products (see Fig. 6).[98] SWNT was suspended with anti-uPA antibody modified ssDNA to produce SWNT sensors that

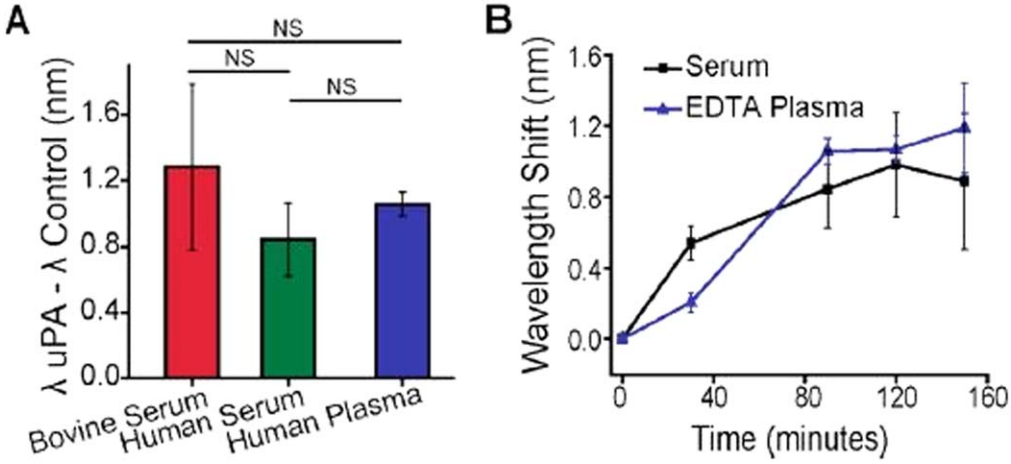

Figure 6. Sensor detection of uPA in human blood products. (A) Addition of 100 nm uPA (ovarian cancer biomarker) to SWNT suspended in bovine serum, human serum, and human plasma all show a distinct red shift in nanotube fluorescence with no solution showing a significantly different shift, indicating consistent detection in various biological media. (B) Red shift of nanotube fluorescence following addition of 100 nm uPA in human serum and human plasma normalized to serum and plasma with no uPA addition, showing a plateu in fluorescence shifting around 90 min (figure reproduced with permission from 98, © 2018 American Chemical Society).

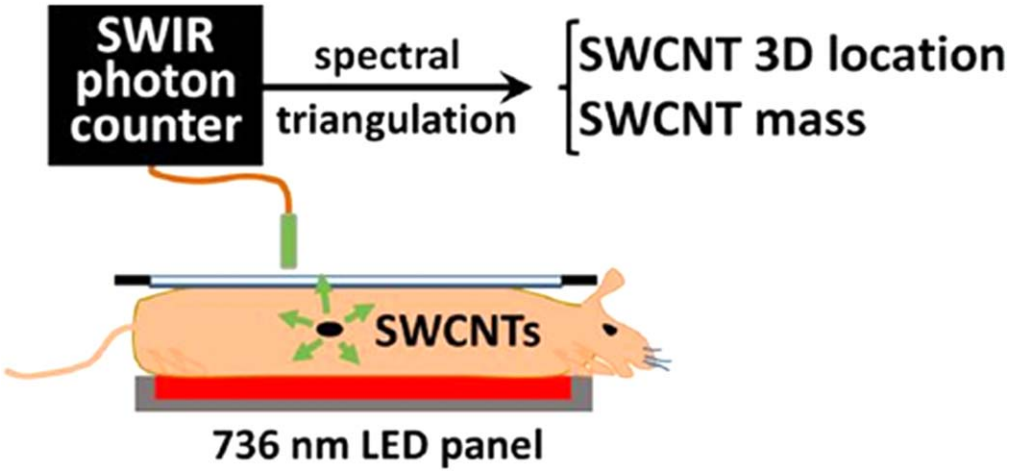

Figure 7. (a) Single walled carbon nanotubes (SWNTs) embedded in Matrigel was imaged in vivo, with the excitation and emission signals located on opposite sides of the mouse (figure reprinted with permission from 100, © 2017 American Chemical Society).

demonstrate a concentration dependent red shift of the fluorescence when exposed to uPA.[98] The red shift response of these sensors was observed in bovine serum, human serum, and human plasma with no significant difference in the response of the sensors to the biomarker.[98] Along the same lines, an HIV detecting SWNT sensor was developed by Harvey et al. using denatured proteins to modulate nanotube response in serum.[99] A ssDNA-based wrapping was used to make the nanotubes specific for intact virus RNA, and it was discovered that denatured proteins help modulate the blue wavelength shift of the sensors due to HIV by interacting with exposed hydrophobic sections along the nanotube.[99]

In vivo.—Advancements with in vivo applications include improved tissue penetration depth, new and improved sensor delivery platforms and increase in the types of analytes that can be detected by SWNT.[100–107]

A major obstacle for SWNT sensors that has been improving over the past three years is detection depth.[100,101] In 2017, Lin et al. functionalized and immobilized SWNT into Matrigel prior to implantation in the mouse ovaries and collection of nIR fluorescence, X-ray and CT data.[100] Spectral triangulation was performed on live mice by using an LED matrix of visible light to excite the SWNT on one side of the animal and a grid of near infrared emission collectors to acquire the signal on the opposing side of the mouse (see Fig. 7).[100] At each position on the emission collection grid, fluorescence intensity was measured through two alternating nIR-II spectral filters, corresponding to weak and strong optical absorption by water in tissues, with a photon counting InGaAs avalanche photodiode. The ratio of the two nIR-II spectral intensities was used to deduce the mass and location of the implanted SWNT. Using this method, Lin et al. has been able to achieve imaging depths of 3.1 mm in vivo and over 10 mm in a tissue phantom despite the small concentration of SWNT used (120 pg in vivo).[100] Bonis-O'Donnell et al. has also increased tissue penetration depth of SWNT sensors by decreasing signal scattering through the use of two-photon excitation on brain tissue phantoms.[101] HiPco nanotubes were suspended with $ss(GT)_{15}$ to create dopamine sensors, which were then loaded into capillary tubes and placed 2 mm deep into brain tissue phantoms.[101] Excitation of the sensors was performed using a two-photon 1560 nm excitation source and showed only a 4% scattering of sensor emission through the tissue mimic, demonstrating the ability of two-photon excitation as a potential deep tissue optical detection method for SWNT sensors.[101]

Sensor delivery plaforms have been another major obstacle in the use of SWNT sensors in vivo. Previous attempts to localize SWNT sensors in hydrogels have resulted in sensor response delays.[85] To address this issue, Hofferber et al. developed two novel hydrogel systems for the localization and real-time detection of biological analytes in vivo (shown in Fig. 8).[102] SWNT sensors for nitric oxide were either encapsulated within a liquid core of a 3D printed hyaluronic acid hydrogel or used to decorate the surface of alginate hydrogels.[102] Both hydrogel-SWNT platforms localized sensors, retained specificity, and maintained function for two months. When the hydrogels were exposed to nitric oxide, SWNT sensors responded in real time with fluorescence quenching.[102] Using a different hydrogel platform, Lee et al. demonstrated the first placement of SWNT sensor implants into large animals, including bony fish, sharks, eels, and turtles.[103] The SWNT sensors were

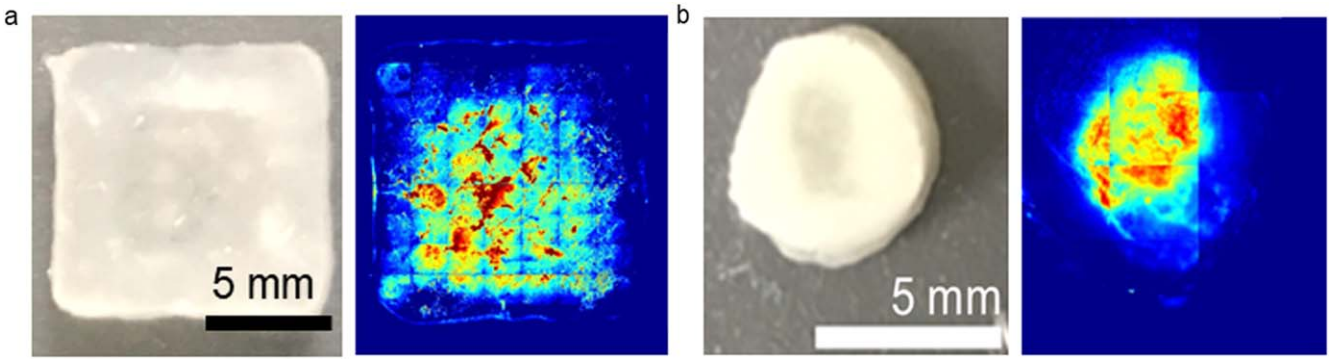

Figure 8. Two hydrogels for in vivo delivery of single walled carbon nanotube (SWNT) sensors that react in real time. (a) 3D printed liquid-core hyaluronic acid hydrogels and (b) alginate hydrogels decorated with SWNT sensors (figure reprinted with permission from 102, © 2019 WILEY-VCH Verlag GmbH & Co. KGaA, Weinheim).

detected at depths of up to 7 mm post sacrifice. Unfortunately, detection of the SWNT signal in live animals was unsuccessful due to animal movement, dispersion of the excitation source, and the long exposure times required by the detector.[103] Despite its inability to detect the sensors in the live animals, this study took the first step in use of SWNT sensors in large animal models.

In vivo detection of various analytes with SWNT sensors has been accomplished in smaller animal models. A sensor for the detection of lipid accumulation in the endolysosomal lumen of mice was developed by Galassi et al.[104] A ssCTTC$_3$TTC wrapped 9,4 SWNT acts as a sensor capable of detecting various lipid species, including cholesterol, sphingomyelin, and oxidized low-density lipoproteins (LDL).[104] The ssCTTC$_3$TTC 9,4 sensors showed in vivo lipid detection and biocompatibility.[104] A sensor for the in vivo detection of ovarian cancer biomarker human epididymis protein 4 (HE4) was developed by Williams et al.[105] The biomarker was shown to be specifically detected by ss(TAT)$_6$-anchored goat polyclonal anti-HE4 immunoglobulin G (IgG) antibody wrapped 9,4 SWNT, relying on a shift in fluorescence wavelength for signal quantification.[105] By wrapping 9,4 SWNT with ss(TAT)$_6$-IgG antibody there is a constant fluorescence intensity that has a concentration dependent blue-shift in response to the presence of HE4.[105] The subcutaneously implanted ss(TAT)$_6$-IgG antibody SWNT was able to demonstrate ovarian cancer biomarker HE4 detection in live mice.[105] Another mouse model by Harvey et al. detected doxorubicin with both subcutaneous and intraperitoneal sensor platforms.[106] DNA suspended nanotubes were found to have a concentration dependent red shift in response to doxorubicin, allowing nondestructive detection of doxorubicin in vivo for the first time.[106] Another exciting breakthrough was performed by Mann et al. when they conjugated SWNT sensors for dopamine to a GFP binding nanobody and introduced the sensors to developing drosophila embryos.[107] The motor protein kinesin-5 was labeled with GFP and aggregation of nanobody-SWNT complexes on the protein was seen upon injection.[107] In this study, the SWNT sensors also remained sensitive to dopamine, showing protein-targeted delivery of a SWNT sensor in vivo.[107]

Conclusions

Single walled carbon nanotubes are small molecules with extraordinary properties, which allows for the development of biosensors for a variety of analytes. The high spatial and temporal resolution of nIR fluorescence in biological samples coupled with the photostability of SWNT has allowed researchers to detect and quantify biomarkers for a number of disease states and many more analytes from biological processes. The field of SWNT as optical biosensors has continued to grow year after year and the library of sensors is rapidly expanding, along with detection methods that are allowing for higher resolution imaging and deeper tissue penetration. There are many hurdles that still need to be overcome before this class of optical biosensors can be used in a clinical setting, including the stigma surrounding their biocompatibility. Early toxicology reports comparing SWNT to asbestos has caused many scientists outside the of the carbon nanotube field to be wary of using nanotube sensors in vivo, but with further characterization of SWNT distribution in vivo, continued improvements in SWNT quantum yield, and improved SWNT sensor delivery platforms the possibility of using SWNT sensors in a clinical setting could become a reality.

References

1. P. Mehrotra, *J. Oral. Biol. Craniofac. Res.*, **6**, 153 (2016).
2. E. M. C. Hillman, C. B. Amoozegar, T. Wang, A. F. H. McCaslin, M. B. Bouchard, J. Mansfield, and R. M. Levenson, *Philos. Trans. A Math Phys. Eng. Sci.*, **369**, 4620 (2011).
3. K. Cammann, *Fresenius J. Anal. Chem.*, **287**, 1 (1977).
4. J. Wang, *Chem. Rev.*, **108**, 814 (2008).
5. E. Akyilmaz, E. Yorganci, and E. Asav, *Bioelectrochemistry*, **78**, 155 (2010).
6. V. Venugopal, *Biosens. Bioelectron.*, **17**, 147 (2002).
7. G. A. Rechnitz, *Chem. Eng. News Arch.*, **56**, 16 (1978).
8. J. Wang, *Biosens. Bioelectron.*, **13**, 757 (1998).
9. V. Scognamiglio, F. Arduini, G. Palleschi, and G. Rea, *TrAC, Trends Anal. Chem.*, **62**, 1 (2014).
10. R. J. Leatherbarrow and P. R. Edwards, *Curr. Opin. Chem. Biol.*, **3**, 544 (1999).
11. X. He, J. Gao, S. S. Gambhir, and Z. Cheng, *Trends Mol. Med.*, **16**, 574 (2010).
12. X. Fan, I. M. White, S. I. Shopova, H. Zhu, J. D. Suter, and Y. Sun, *Anal. Chim. Acta*, **620**, 8 (2008).
13. Y. Liu, X. Dong, and P. Chen, *Chem. Soc. Rev.*, **41**, 2283 (2012).
14. E. Katz and I. Willner, *Electroanalysis*, **15**, 913 (2003).
15. P. Jiang and Z. Guo, *Coord. Chem. Rev.*, **248**, 205 (2004).
16. T. Kuila, S. Bose, P. Khanra, A. K. Mishra, N. H. Kim, and J. H. Lee, *Biosens. Bioelectron.*, **26**, 4637 (2011).
17. Y. Cai, Z. Wei, C. Song, C. Tang, W. Han, and X. Dong, *Chem. Soc. Rev.*, **48**, 22 (2019).
18. M. A. Cooper, *Nat. Rev. Drug Discovery*, **1**, 515 (2002).
19. M. Seydack, *Biosens. Bioelectron.*, **20**, 2454 (2005).
20. D. A. Heller, H. Jin, B. M. Martinez, D. Patel, B. M. Miller, T.-K. Yeung, P. V. Jena, C. Höbartner, T. Ha, and S. K. Silverman, *Nat. Nanotechnol.*, **4**, 114 (2009).
21. S. Diao, G. Hong, J. T. Robinson, L. Jiao, A. L. Antaris, J. Z. Wu, C. L. Choi, and H. Dai, *JACS*, **134**, 16971 (2012).
22. H. Yi, D. Ghosh, M.-H. Ham, J. Qi, P. W. Barone, M. S. Strano, and A. M. Belcher, *Nano Lett.*, **12**, 1176 (2012).
23. K. Welsher, S. P. Sherlock, and H. Dai, *Proc. Natl Acad. Sci. USA*, **108**, 8943 (2011).
24. G. Hong, J. C. Lee, J. T. Robinson, U. Raaz, L. Xie, N. F. Huang, J. P. Cooke, and H. Dai, *Nat. Med.*, **18**, 1841 (2012).
25. J. T. Robinson, G. Hong, Y. Liang, B. Zhang, O. K. Yaghi, and H. Dai, *JACS*, **134**, 10664 (2012).
26. J. Zhang, R. E. Campbell, A. Y. Ting, and R. Y. Tsien, *Nat. Rev. Mol. Cell Biol.*, **3**, 906 (2002).
27. J. Lippincott-Schwartz and G. H. Patterson, *Science*, **300**, 87 (2003).
28. N. C. Shaner, P. A. Steinbach, and R. Y. Tsien, *Nat. Methods*, **2**, 905 (2005).
29. R. Y. Tsien, *FEBS Lett.*, **579**, 927 (2005).
30. B. N. G. Giepmans, S. R. Adams, M. H. Ellisman, and R. Y. Tsien, *Science*, **312**, 217 (2006).
31. A. Ibraheem and R. E. Campbell, *Curr. Opin. Chem. Biol.*, **14**, 30 (2010).
32. B. Wu, K. D. Piatkevich, T. Lionnet, R. H. Singer, and V. V. Verkhusha, *Curr. Opin. Cell Biol.*, **23**, 310 (2011).
33. N.-N. Aye-Han, Q. Ni, and J. Zhang, *Curr. Opin. Chem. Biol.*, **13**, 392 (2009).
34. A. M. Smith, M. C. Mancini, and S. Nie, *Nat. Nanotechnol.*, **4**, 710 (2009).
35. T. Durduran, R. Choe, W. B. Baker, and A. G. Yodh, *Rep. Prog. Phys.*, **73**, 076701 (2010).
36. B. Chance, *Ann. N.Y. Acad. Sci.*, **838**, 29 (1998).
37. R. R. Anderson and J. A. Parrish, *J. Investig. Dermatol.*, **77**, 13 (1981).
38. H. Zhang, D. Salo, D. M. Kim, S. Komarov, Y.-C. Tai, and M. Y. Berezin, *J. Biomed. Opt.*, **21**, 126006 (2016).
39. G. Chen, I. Roy, C. Yang, and P. N. Prasad, *Chem. Rev.*, **116**, 2826 (2016).
40. E. Hemmer, A. Benayas, F. Légaré, and F. Vetrone, *Nanoscale Horizons*, **1**, 168 (2016).
41. S. Arai, K. Kirihata, M. Shimizu, M. Ueda, A. Katada, and M. Uejima, *J. Electrochem. Soc.*, **164**, D922 (2017).
42. H. Wu, T. Wei, X. Li, J. Yang, J. Zhang, S. Fan, and H. Zhang, *J. Electrochem. Soc.*, **164**, B147 (2017).
43. J. Zhuang, X. Jiang, J. Wang, C. Yang, and H. Yang, *J. Electrochem. Soc.*, **164**, H1028 (2017).
44. A. S. Ahammad, T. Akter, A. Al Mamun, T. Islam, M. M. Hasan, M. Mamun, S. Faraezi, F. Monira, and J. K. Saha, *J. Electrochem. Soc.*, **165**, B390 (2018).
45. T. V. Kumar and A. K. Sundramoorthy, *J. Electrochem. Soc.*, **165**, B3006 (2018).
46. A. G. Zestos and B. J. Venton, *J. Electrochem. Soc.*, **165**, G3071 (2018).
47. S. Iijima, *Nature*, **354**, 56 (1991).
48. R. Zhang, Y. Zhang, Q. Zhang, H. Xie, W. Qian, and F. Wei, *ACS Nano*, **7**, 6156 (2013).
49. R. D. Saito, G. Dresselhaus, and M. S. Dresselhaus, in *Physical Properties of Carbon Nanotubes* (Singapore, World Scientific) 35–58 (1998).
50. M. Zheng, *Top. Curr. Chem. (Cham)*, **375**, 13 (2017).
51. S. M. Bachilo, M. S. Strano, C. Kittrell, R. H. Hauge, R. E. Smalley, and R. B. Weisman, *Science*, **298**, 2361 (2002).
52. S. A. Hodge, M. K. Bayazit, K. S. Coleman, and M. S. P. Shaffer, *Chem. Soc. Rev.*, **41**, 4409 (2012).
53. A. V. Naumov, O. A. Kuznetsov, A. R. Harutyunyan, A. A. Green, M. C. Hersam, D. E. Resasco, P. N. Nikolaev, and R. B. Weisman, *Nano Lett.*, **9**, 3203 (2009).
54. J. W. G. Wilder, L. C. Venema, A. G. Rinzler, R. E. Smalley, and C. Dekker, *Nature*, **391**, 59 (1998).
55. M. J. O'Connell et al., *Science*, **297**, 593 (2002).
56. A. Jorio, M. A. Pimenta, A. G. S. Filho, R. Saito, G. Dresselhaus, and M. S. Dresselhaus, *New J. Phys.*, **5**, 139 (2003).
57. S. Kruss, A. J. Hilmer, J. Zhang, N. F. Reuel, B. Mu, and M. S. Strano, *Adv. Drug Delivery Rev.*, **65**, 1933 (2013).
58. Z. Liu, S. Tabakman, K. Welsher, and H. Dai, *Nano Res.*, **2**, 85 (2009).
59. R. A. Graff, J. P. Swanson, P. W. Barone, S. Baik, D. A. Heller, and S. M. Strano, *Adv. Mater.*, **17**, 980 (2005).
60. H. Kuzmany, B. Burger, M. Fally, A. G. Rinzler, and R. E. Smalley, *Physica B*, **244**, 186 (1998).
61. S. Diao, G. Hong, A. L. Antaris, J. L. Blackburn, K. Cheng, Z. Cheng, and H. Dai, *Nano Res.*, **8**, 3027 (2015).
62. S. S. Wong, E. Joselevich, A. T. Woolley, C. L. Cheung, and C. M. Lieber, *Nature*, **394**, 52 (1998).

63. N. W. S. Kam, M. O'Connell, J. A. Wisdom, and H. Dai, *Proc. Natl Acad. Sci. USA*, **102**, 11600 (2005).
64. W. Wu, S. Wieckowski, G. Pastorin, M. Benincasa, C. Klumpp, J. P. Briand, R. Gennaro, M. Prato, and A. Bianco, *Angew. Chem. Int. Ed. Engl.*, **44**, 6358 (2005).
65. Z. Liu, C. Davis, W. Cai, L. He, X. Chen, and H. Dai, *Proc. Natl Acad. Sci.*, **105**, 1410 (2008).
66. Z. Liu, X. Sun, N. Nakayama-Ratchford, and H. Dai, *ACS Nano*, **1**, 50 (2007).
67. M. L. Schipper, N. Nakayama-Ratchford, C. R. Davis, N. W. S. Kam, P. Chu, Z. Liu, X. Sun, H. Dai, and S. S. Gambhir, *Nat. Nanotechnol.*, **3**, 216 (2008).
68. K. Welsher, Z. Liu, S. P. Sherlock, J. T. Robinson, Z. Chen, D. Daranciang, and H. Dai, *Nat. Nanotechnol.*, **4**, 773 (2009).
69. H. Dumortier, S. Lacotte, G. Pastorin, R. Marega, W. Wu, D. Bonifazi, J. P. Briand, M. Prato, S. Muller, and A. Bianco, *Nano Lett.*, **6**, 1522 (2006).
70. X. Chen, U. C. Tam, J. L. Czlapinski, G. S. Lee, D. Rabuka, A. Zettl, and C. R. Bertozzi, *JACS*, **128**, 6292 (2006).
71. S. F. Chin, R. H. Baughman, A. B. Dalton, G. R. Dieckmann, R. K. Draper, C. Mikoryak, I. H. Musselman, V. Z. Poenitzsch, H. Xie, and P. Pantano, *Exper. Biol. Med.*, **232**, 1236 (2007).
72. H. N. Yehia, R. K. Draper, C. Mikoryak, E. K. Walker, P. Bajaj, I. H. Musselman, M. C. Daigrepont, G. R. Dieckmann, and P. Pantano, *J. Nanobiotechnol.*, **5**, 8 (2007).
73. J. Zhang et al., *JACS*, **133**, 567 (2011).
74. P. Cherukuri, C. J. Gannon, T. K. Leeuw, H. K. Schmidt, R. E. Smalley, S. A. Curley, and R. B. Weisman, *Proc. Natl Acad. Sci. USA*, **103**, 18882 (2006).
75. A. A. Boghossian et al., *Chem. Sus. Chem.*, **4**, 848 (2011).
76. P. Cherukuri, S. M. Bachilo, S. H. Litovsky, and R. B. Weisman, *JACS*, **126**, 15638 (2004).
77. D. A. Heller, R. M. Mayrhofer, S. Baik, Y. V. Grinkova, M. L. Usrey, and M. S. Strano, *JACS*, **126**, 14567 (2004).
78. J. Lefebvre, J. Fraser, P. Finnie, and Y. Homma, *Phys. Rev. B*, **69**, 075403 (2004).
79. Z. Ren, Z. Huang, J. Xu, J. Wang, P. Bush, M. Siegal, and P. Provencio, *Science*, **282**, 1105 (1998).
80. W. Li, S. Xie, L. Qian, B. Chang, B. Zou, W. Zhou, R. Zhao, and G. Wang, *Science*, **274**, 1701 (1996).
81. S. Giordani, S. D. Bergin, V. Nicolosi, S. Lebedkin, M. M. Kappes, W. J. Blau, and J. N. Coleman, *J. Phys. Chem. B*, **110**, 15708 (2006).
82. T. K. Leeuw, R. M. Reith, R. A. Simonette, M. E. Harden, P. Cherukuri, D. A. Tsyboulski, K. M. Beckingham, and R. B. Weisman, *Nano Lett.*, **7**, 2650 (2007).
83. L. Cognet, D. A. Tsyboulski, J.-D. R. Rocha, C. D. Doyle, J. M. Tour, and R. B. Weisman, *Science*, **316**, 1465 (2007).
84. F. A. Mann, N. Herrmann, D. Meyer, and S. Kruss, *Sensors (Basel)*, **17**, 1521 (2017).
85. N. M. Iverson, P. W. Barone, M. Shandell, L. J. Trudel, S. Sen, F. Sen, V. Ivanov, E. Atolia, E. Farias, and T. P. McNicholas, *Nat. Nanotechnol.*, **8**, 873 (2013).
86. A. G. Beyene, A. A. Alizadehmojarad, G. Dorlhiac, N. Goh, A. M. Streets, P. Král, L. Vuković, and M. P. Landry, *Nano Lett.*, **18**, 6995 (2018).
87. J. D. Harvey, H. A. Baker, E. Mercer, J. Budhathoki-Uprety, and D. A. Heller, *ACS Appl. Mater. Interfaces*, **9**, 37947 (2017).
88. K. Lee, J. Lee, and B. Ahn, *Anal. Chem.*, **91**, 12704 (2019).
89. V. Zubkovs, N. Schuergers, B. Lambert, E. Ahunbay, and A. A. Boghossian, *Small*, **13**, 1701654 (2017).
90. J. Dong, D. P. Salem, J. H. Sun, and M. S. Strano, *ACS Nano*, **12**, 3769 (2018).
91. S. Kruss, D. P. Salem, L. Vuković, B. Lima, E. Vander Ende, E. S. Boyden, and M. S. Strano, *Proc. Natl Acad. Sci.*, **114**, 1789 (2017).
92. M. Dinarvand, E. Neubert, D. Meyer, G. Selvaggio, F. A. Mann, L. Erpenbeck, and S. Kruss, *Nano Lett.*, **19**, 6604 (2019).
93. L. Chio, J. T. Del Bonis-O'Donnell, M. A. Kline, J. H. Kim, I. R. McFarlane, R. N. Zuckermann, and M. P. Landry, *Nano Lett.*, **19**, 7563–72 (2019).
94. J. Budhathoki-Uprety, R. E. Langenbacher, P. V. Jena, D. Roxbury, and D. A. Heller, *ACS Nano*, **11**, 3875 (2017).
95. G. Bisker, N. A. Bakh, M. A. Lee, J. Ahn, M. Park, E. B. O'Connell, N. M. Iverson, and M. S. Strano, *ACS Sensors*, **3**, 367 (2018).
96. M. P. Landry, H. Ando, A. Y. Chen, J. Cao, V. I. Kottadiel, L. Chio, D. Yang, J. Dong, T. K. Lu, and M. S. Strano, *Nat. Nanotechnol.*, **12**, 368 (2017).
97. J. Budhathoki-Uprety et al., *Nat. Commun.*, **10**, 1 (2019).
98. R. M. Williams, C. Lee, and D. A. Heller, *ACS Sensors*, **3**, 1838 (2018).
99. J. D. Harvey, H. A. Baker, M. V. Ortiz, A. Kentsis, and D. A. Heller, *ACS Sensors*, **4**, 1236 (2019).
100. C.-W. Lin, H. Yang, S. R. Sanchez, W. Mao, L. Pang, K. M. Beckingham, R. C. BastJr, and R. B. Weisman, *ACS Appl. Mater. Interfaces*, **9**, 41680 (2017).
101. J. T. D. Bonis-O'Donnell, R. H. Page, A. G. Beyene, E. G. Tindall, I. R. McFarlane, and M. P. Landry, *Adv. Funct. Mater.*, **27**, 1702112 (2017).
102. E. M. Hofferber, J. A. Stapleton, J. Adams, M. Kuss, B. Duan, and N. M. Iverson, *Macromol. Biosci.*, **19**, 1800469 (2019).
103. M. A. Lee, F. T. Nguyen, K. Scott, N. Y. Chan, N. A. Bakh, K. K. Jones, C. Pham, P. Garcia-Salinas, D. Garcia-Parraga, and A. Fahlman, *ACS sensors*, **4**, 32 (2018).
104. T. V. Galassi et al., *Sci. Transl. Med.*, **10**, eaar2680 (2018).
105. R. M. Williams et al., *Sci. Adv.*, **4**, eaaq1090 (2018).
106. J. D. Harvey, R. M. Williams, K. M. Tully, H. A. Baker, Y. Shamay, and D. A. Heller, *Nano Lett.*, **19**, 4343 (2019).
107. F. A. Mann, Z. Lv, J. Großhans, F. Opazo, and S. Kruss, *Angew. Chem. Int. Ed.*, **58**, 11469 (2019).